

1 **Histopathological assessments reveal retinal vascular changes, inflammation and gliosis in patients**
2 **with lethal COVID-19**

3 Vijay K. Jidigam, PhD¹, Rupesh Singh, PhD¹, Julia C. Batoki¹, Caroline Milliner¹, Onkar B. Sawant,
4 PhD², Vera L. Bonilha, PhD^{1,3}, Sujata Rao, PhD^{1,3}.

5 ¹ Department of Ophthalmic Research, Cole Eye Institute, Cleveland Clinic, 9500 Euclid Avenue,
6 Cleveland, OH;

7 ² Center for Vision and Eye Banking Research, Eversight, 6700 Euclid Ave, Suite 101, Cleveland, OH;

8 ³ Department of Ophthalmology, Cleveland Clinic Lerner College of Medicine of Case Western Reserve
9 University, Cleveland, OH

10 **Corresponding Authors:** Sujata Rao, PhD and Vera L. Bonilha, PhD.

11 **Financial Support:** This research was funded by grants from the U.S. National Institutes of
12 Health/National Eye Institute EY027077-01 (S.R.), RPB1503 (S.R.), EY027750 (VLB), a National Eye
13 Institute P30-EY025585 Core Grant, a Cleveland Eye Bank Foundation Grant awarded to the Cole Eye
14 Institute, and Research to Prevent Blindness Challenge Grant. Research activities at Eversight are supported
15 by funding from LC Industries (Durham, NC), Eye Bank Association of America and Connecticut Lions
16 Eye Research Foundation. The funding organizations had no role in the design or the conduct of this
17 research.

18 **Conflict of Interest:** No conflicting relationship exists for any author.

19 **Running head:** Vascular and inflammatory changes in patients with lethal COVID-19.

20 **Address for reprints:** Department of Ophthalmic Research, Cole Eye Institute, Cleveland Clinic, 9500
21 Euclid Avenue, Cleveland, OH, 44195 (raos7@ccf.org and bonilhav@ccf.org)

22 **Key Words:** COVID-19, Retina, histopathology, vasculature, inflammation

23 **ABSTRACT**

24 **Purpose:** To assess for histopathological changes within the retina and the choroid and determine the
25 long-term sequelae of the SARS-CoV-2 infection.

26 **Design:** Comparative analysis of human eyes.

27 **Subjects:** Eleven donor eyes from COVID-19 positive donors and similar age-matched donor eyes from
28 patients with a negative test for SARS-CoV-2 were assessed.

29 **Methods:** Globes were evaluated ex-vivo with macroscopic, SLO and OCT imaging. Macula and
30 peripheral regions were processed for epon-embedding and immunocytochemistry

31 **Main Outcome Measures:** Retinal thickness and histopathology, detection of SARS-CoV-2 Spike
32 protein, changes in vascular density, gliosis, and degree of inflammation.

33 **Results:** Fundus analysis shows hemorrhagic spots and increased vitreous debris in several of the
34 COVID-19 eyes compared to the control. OCT based measurements indicated an increased trend in
35 retinal thickness in the COVID-19 eyes, however the difference was not statistically significant.
36 Histology of the retina showed presence of hemorrhages and central cystoid degeneration in several of the
37 donors. Whole mount analysis of the retina labeled with markers showed changes in retinal
38 microvasculature, increased inflammation, and gliosis in the COVID-19 eyes compared to the controls.
39 The choroidal vasculature displayed localized changes in density and signs of increased inflammation in
40 the COVID-19 samples.

41 **Conclusions:** *In situ* analysis of the retinal tissue suggested that there are severe subclinical abnormalities
42 that could be detected in the COVID-19 eyes. This study provides a rationale for evaluating the ocular
43 physiology of patients that have recovered from COVID-19 infections to further understand the long-term
44 effects caused by this virus.

45

46 INTRODUCTION

47 We are amid the human coronavirus disease 2019 (COVID-19) pandemic, caused by severe acute
48 respiratory syndrome coronavirus (SARS-CoV-2), which is of historic proportions, the likes of which we
49 have not seen in 102 years. With >25 million cases confirmed, >490K deaths in the US (WHO COVID-
50 19 Dashboard) it is one of the deadliest events in US history, and rates continuing to rise, the end is not in
51 near sight. Despite being primarily a respiratory virus, COVID-19 can also present with non-respiratory
52 signs, including ocular symptoms as conjunctival hyperemia, chemosis, epiphora, increased secretions,
53 ocular pain, photophobia, and dry eye¹⁻⁶. SARS-CoV-2 requires host cellular receptors (such as ACE2)
54 for successful replication during infections. Immuno-histochemical studies and single-cell RNA-
55 sequencing datasets have revealed both extra- and intra-ocular localization of SARS-CoV-2 receptors
56 ACE2 receptor, and TMPRSS2 protease in human eyes^{1,7-9}. The virus has also been detected within the
57 anterior chamber and in the ocular fluids suggesting that ocular tissue may be directly affected due to
58 Sars-CoV-2 infection^{1,10,11}. Evidence of posterior eye involvement¹ in SARS-COV-2 infection is still
59 scarce, though some recent optical coherence tomography angiography (OCTA) based findings show that
60 retinal microvasculature is affected in patients that recovered from COVID-19 infection^{12,13}. However, a
61 detailed histopathological analysis of the retinal tissue and the impact of the SARS-CoV-2 infection on
62 ocular health and function has not been examined. Here we report a comprehensive analysis of eyes from
63 post-mortem patients infected with the SARS-CoV-2 virus. Fundus imaging provides evidence of
64 increased hemorrhage in the eyes of COVID-19 patients. In some SARS-CoV-2 positive patients, there
65 was evidence of vascular anomalies consistent with ocular vein occlusion and reduced capillary density.
66 Additionally, there is an overall increase in the number of microglial cells within the retina of COVID-19
67 patients. The microglial cells display abnormal morphological features indicative of microglial dystrophy.
68 There is also increased gliosis in the COVID-19 eyes compared to the eyes from the age-matched control
69 donors. To our knowledge, this is the first study that provides in vivo molecular information concerning
70 the changes occurring within the retinal tissue of COVID-19 patients. We are still in the midst of the

71 coronavirus outbreak and there is constantly emerging information regarding its long-term sequelae on
72 various systems in the body. The data reported here provide a rationale for longitudinal ocular
73 assessments in recovered patients to truly gain insights into understanding the long-term effects caused by
74 this virus.

75

76 **METHODS**

77 **Tissue acquisition and fixation**

78 Donor eyes were obtained through Eversight (Cleveland, OH). Eye bank records accompanying the donor
79 eyes indicated whether the donor had COVID-19. Pathology analysis was performed with the approval of
80 the Cleveland Clinic Institutional Review Board (IRB #20-755) and Institutional Biosafety Committee
81 (IBC# 2018). The research adhered to the tenets of the Declaration of Helsinki. Tissue from eleven
82 COVID-19 donor eyes from seven donors was analyzed. Additional information about the donors is
83 provided in Table 1 (Fig 1). Cornea and anterior segment analysis for the COVID-19 donors were
84 recently reported by Sawant et al.¹¹ For analysis, globes without the cornea were fixed and kept in 4%
85 paraformaldehyde and 0.5% glutaraldehyde made in Dulbecco's Phosphate Buffered Saline (D-PBS)
86 buffer for at least a month.

87

88 **Ex-vivo imaging of globes**

89 Globes were cut through the ora serrata, posterior poles were transferred to a chamber filled with D-PBS
90 solution and imaged as previously described¹⁴. Briefly, fundus macrophotography (FM) images were
91 collected using a Zeiss AxioCam MRC5 camera equipped with a macro zoom lens and AxioVision AC
92 Software (Zeiss). Fundus autofluorescence was obtained using Blue Autofluorescence (BAF) mode of
93 Heidelberg Spectralis confocal scanning laser ophthalmoscopy (SLO) (Heidelberg Engineering, Inc.).
94 Optical Coherence Tomography images (OCT) were collected using spectral domain OCT system
95 (Envisu R2210 UHR Leica Microsystems Inc.).

96 **Histopathology**

97 Fragments of retina-RPE-choroid were cut from the periphery to the optic nerve head and placed in 2.5%
98 glutaraldehyde in 0.1M cacodylate buffer, sequentially dehydrated in ethanol and embedded in Epon as
99 previously reported¹⁵. For light microscopy, semi-thin sections were cut with a diamond histotech knife,
100 dried, and stained with toluidine blue. Slides were photographed with a Zeiss AxioImager.Z1 light
101 microscope and the images were digitized using a Zeiss AxioCam MRc5 camera.

102

103 **Retinal flatmount and immunohistochemistry**

104 A piece of retina and choroid were cut from the posterior pole of each eyecup. The retina was dissected
105 and washed overnight in TBS. The RPE/choroid was incubated in the disodium salt of
106 ethylenediaminetetraacetic acid for 1.5 hours and RPE was removed using a pipette before washing with
107 TBS overnight and wholemount staining was performed as described with the exception that the tissues
108 were incubated with the antibodies and the UEA lectin for 4 days¹⁶. Retinas were stained with chicken
109 anti-glial fibrillary acidic protein (GFAP; 1:500; Millipore, Burlington, MA, USA), mouse anti- SARS-
110 CoV S Protein (1:100; NR-614, BEI Resources, NIAID, Manassas, VA, USA), rabbit anti-Iba-1 (1:250;
111 Wako Chemicals USA, Inc., Richmond, VA) and Ulex europaeus agglutinin-FITC (UEA lectin1:100;
112 Genetex, Irvine, CA, USA). Choroids were stained with UEA Lectin and Iba-1 antibody. The submacular
113 regions of the retina were imaged using a Leica confocal microscope. Retinal images were acquired from
114 three different zones, one near the ONH and Vein, one near the middle and one towards the periphery^{17,18}.
115 All care was taken to ensure that similar regions were represented in the images. The choroids were
116 imaged with Bruch's membrane proximal to the objective.

117

118 **RESULTS**

119 **Imaging of posterior globes**

120 The combination of the fundus, confocal scanning laser ophthalmoscopy and optical coherence
121 tomography imaging systems can provide a comprehensive characterization of retinal lesions before
122 histopathology¹⁹. Therefore, these imaging techniques were performed on all COVID-19 and control eye
123 donors; images obtained were qualitatively compared (Fig 1). Anatomical landmarks such as the optic
124 nerve (ON) and fovea (Fig 1, black arrows) were identified in all donor's eyes using all three imaging
125 modalities. Fundus images displayed differences between the eyes from both groups, which included
126 several hemorrhage spots in the COVID-19 eyes (Fig 1A to 1F, white arrowheads). SLO BAF imaging
127 revealed detached retina areas in the COVID-19 eyes (Fig 1H, 1J, and 1L, asterisks); further studies are
128 needed to understand the cause of these retinal detachment areas. In addition, hemorrhage spots in the
129 COVID-19 eyes were observed as hypofluorescent spots (Fig 1H, 1J, and 1L, white arrowheads).
130 Quantification of SLO images showed decreased BAF signal in the COVID-19 eyes compared to
131 controls, but the increase was not significant (Fig 1M to 1P). Finally, OCT based measures for retinal
132 thickness and optic nerve head depth showed slight increase in the COVID-19 eyes compared to controls,
133 but the increase was not significant (Supplemental Fig S1). In general, COVID-19 posterior poles had
134 more vitreous debris, most likely due to detached epiretinal membranes or cellular floaters.

135

136 **Histopathological and immunohistological findings in the retina of COVID-19 patients**

137 Little is known about the ocular implications of COVID-19 disease. To gain insight into the disease's
138 retinal pathology, semi-thin sections of epon-embedded tissue were analyzed and compared to matched
139 controls. The control donors' retinas displayed each of the usual retinal lamina and the RPE (Fig 2A). The
140 COVID-19 donors' retina displayed retinal edema compared to the control retinas (Fig 2B). Interestingly,
141 a few control retinas displayed variable areas of cystoid change and atrophy in the retina's far periphery
142 (Fig 2C). However, cystoid changes and atrophies were observed in the central area of the COVID-19
143 donors (Fig 2D). In our cohort of COVID-19 samples, we also observed hemorrhages of various sizes in
144 the outer plexiform layer around the optic nerve head in a few COVID-19 donors (Fig 2E and F,
145 asterisks); these were also autofluorescent in cryosections. The frequency of observed morphological

146 findings detected in our cohort is provided in Table 2. Immunostaining of retinas with SARS-CoV-2 S
147 protein antibody reacted with round cells within the retina of all the COVID-19 eyes close to the optic
148 nerve head but not in the control retinas. However, in the retinas of two of the COVID-19 positive cases
149 several cells were identified in the retina, choroid and optic nerve head (Fig 2H, and 2I, arrows) but not in
150 the controls.

151

152 **Retinal microvasculature anomalies in COVID-19 patients:**

153 To gain insight into the disease's retinal pathology, flatmounts of both retina and choroid were labeled
154 with a lectin that labels the endothelium of vessels. In 4 out of 7 COVID-19 positive donor eyes, there
155 were signs of major vein occlusion, indicated by constriction of the vein and increased signs of
156 hemorrhages upstream of the constrictions (Supplemental Fig S2). Additionally, in the COVID-19
157 positive eyes, microvasculature density was severely reduced closer to the optic disc and around the veins
158 (Fig 3A to 3F) compared to the age-matched control donor eyes. In several of the COVID-19 eyes, there
159 was an observable loss of microvasculature and distinct thinning of the microcapillaries compared to the
160 control eyes. In the choroidal plexus, vasculature did not appear to be different between the COVID-19
161 eyes and the age matched control cohorts. Though in some areas there was reduced focal lectin staining
162 indicative of capillary dropouts unlike in the retinal vasculature, it was difficult to determine whether
163 there is an overall reduction in the choroidal vasculature density in the COVID-19 patients (Supplemental
164 Fig S3). Nevertheless, our analysis suggests that there are distinct histological changes in the retinal
165 microvasculature. Though it is not possible to conclusively determine whether all reported vascular
166 features can be completely attributed to the virus, based on the comparative analysis of the age-matched
167 control donor eyes, it is important to note that other comorbidities cannot solely explain the observed
168 differences.

169 **Gliosis and increased infiltration of microglial cells in the retina of COVID-19 patients.**

170 SARS-CoV-2 infection can lead to multisystem inflammatory syndrome. Ocular tissue, like many other
171 tissues can be affected by this inflammatory process. To determine whether signs of increased
172 inflammation can be detected, we assessed for gliosis and inflammation in the retina of COVID-19
173 patients. Retinal and choroidal preparations were examined using GFAP, a marker for astrocytes (Fig 4A
174 to 4L) and Iba-1, to label the microglial cells (Fig 4A' to 4L'). Irrespective of whether the eyes were from
175 COVID-19 positive or negative individuals, Iba-1 positive microglial cells could be detected in all the
176 eyes. As a result of aging, an increasing proportion of microglial cells display abnormal morphological
177 features such as shortened, gnarled, beaded, or fragmented cytoplasmic processes, and loss of fine
178 ramifications and formation of spheroidal swellings; these changes are designated collectively as
179 microglial dystrophy²⁰. These changes are determined to be different than what occurs during microglial
180 activation which is defined as hypertrophic microglia²⁰⁻²³. In all the eyes examined, there was evidence
181 for both hypertrophic and dystrophic microglia, though there was evidence of microglial dystrophy in
182 more of the COVID-19 eyes compared to the controls. (Fig 4E'-4L', hypertrophic are indicated with red
183 arrow heads, while dystrophic features are indicated with blue and yellow arrowheads; magenta is normal
184 morphology) Additionally, in all the COVID-19 eyes examined, there was also an overall increase in the
185 number of microglial cells (Fig 4C', 4D', 4G', 4H', 4K', 4L'). This increase was observed closer to the
186 optic nerve head and towards the middle and the peripheral retina. An overall assessment of the increased
187 microglial cells is also indicated in Table 2. Besides the differences in the numbers, microglial cells also
188 displayed activated microglia characteristics with enlarged spheroidal morphology and retracted
189 processes. Similar to our retinal observations, there was evidence of increased microglial cells in the
190 choroid (Supplemental Fig S2). A direct or systemic inflammation can result in the activation of the
191 astrocytes along with the microglial cells. Astrocyte network were visualized with GFAP. GFAP
192 immunoreactivity was highly variable with temporal differences within macular and perimacular regions
193 that were examined. In general, closer to the optic nerve, the GFAP immunoreactivity was increased in
194 the COVID-19 patients compared to their age matched controls. The astrocyte networks also appear to be
195 different, with more elongated cell processes closer to the ONH (Fig 4C, 4G,4K) but towards the mid and

196 peripheral regions, these elongated bundles appear to overlap and form dense mesh like structures (Fig
197 4D,4H, 4L). The increased GFAP immunoreactivity suggests signs of increased gliosis within the retina
198 of patients infected with SARS-CoV-2 virus. However, due to the limited number of eyes examined, it is
199 difficult to conclusively assess the influences of other comorbidities such as age and sex for the analysis.

200

201 **DISCUSSION**

202 Though the SARS-CoV-2 is primarily a respiratory tract virus, there is sufficient evidence that the virus
203 can be detected in several other tissues like the peripheral and central nervous systems. The presence of
204 the ACE2 receptor and the cofactor TMPRSS2 in several anatomical parts of the anterior surface suggest
205 that the SAR-CoV-2 infection of the eye tissues, especially at the limbus and the cornea is possible. In
206 agreement with this observation, a recent report estimated the prevalence of ocular manifestations in
207 COVID-19 patients to range between 2 to 32%²⁴. The ophthalmic manifestations appear to be associated
208 with the disease severity of COVID-19^{1,25}. Several groups have reported varying viral RNA and protein
209 levels within the tears, conjunctiva, cornea, and vitreous^{11,26}. The presence of viral ribonucleic acid
210 (RNA) of SARS-CoV-2 was reported in three of fourteen human retinas of deceased patients with
211 confirmed COVID-19 by real-time reverse transcriptase-polymerase chain reaction (RT-PCR)²⁷. In this
212 study, SARS-CoV-2 S protein immunoreactivity showed different degrees of distinct and specific
213 localization in round cells within the retina of all the COVID-19 eyes close to the optic nerve head. The
214 anterior segments of our COVID-19 cohort's eyes were previously analyzed¹¹. Among eleven eyes
215 recovered from seven COVID-19 donors: three conjunctival, one anterior corneal, five posterior corneal,
216 and three vitreous swabs tested positive for SARS-CoV-2 RNA. Cases of SARS-CoV-2 have been known
217 to induce anterior segment pathologies such as conjunctivitis and anterior uveitis and posterior
218 pathologies, including retinitis, optic neuritis, choroiditis with retinal detachment and retinal

219 vasculitis^{25,28}. These studies further illustrate the importance of long-term assessments of ocular
220 physiology of individuals that have recovered from COVID-19.

221 To date, there is no detailed cellular and molecular characterization of the retina in SARS-CoV-2 infected
222 patients. Previous studies reported retinal lesions in outpatients after confirmed SARS-CoV-2 infection
223 with mild to moderate symptoms. Findings included non-specific and controversial hyper-reflective OCT
224 lesions in the ganglion cell and inner plexiform layers, microhemorrhages, and nerve fiber infarcts²⁹.
225 Other studies identified hemorrhages, cotton wool spots, dilated veins and tortuous vessels in fundus
226 photographs^{13,30}. These are commonly seen as manifestations of diabetes mellitus and systemic
227 hypertension but are also associated with several other etiologies, including ischemic, embolic,
228 connective tissue, neoplastic, and infectious³¹⁻³³. CWSs compromise localized accumulations of
229 axoplasmic debris at the level of retinal ganglion cell axons resulting from axoplasmic flow interruption
230 due to vascular or mechanical causes³⁴. In our histological study, we detected amorphous debris in the
231 outer plexiform layer corresponding to hemorrhages. Another exciting finding observed in COVID-19
232 eyes was the presence of a large number of cystoid lesions spread across the entire retina that closely
233 resemble the retinal alterations of patients suffering from cystoid macular edema (CME)^{35,36} is observed
234 in human retinal diseases like AMD, diabetic retinopathy, retinal vein occlusion, retinitis pigmentosa^{35,37},
235 optic atrophy³⁸, among others^{36,39}. The presence of cysts causes a thickening of the affected retina and
236 decreases visual acuity. Moreover, the neuroretina's compression, the nerve fibers and capillaries by the
237 cystic alterations further contribute to retinal degeneration and aggravation of hypoxic conditions.

238 Though, data on histopathological analysis of retinal vasculature and choriocapillaris is scarce,
239 there have been a few studies on OCTA based findings in patients with SARS-Cov-2. In a recent study by
240 Abrishami et al,¹² OCTA was performed 2 weeks after recovery from systemic COVID-19 and mean
241 vessel density in the superficial and deep plexus were significantly reduced in the COVID-19 cohort
242 versus the age matched controls. In another study by Turker et al⁴⁰, a reduction in retinal vessel density of
243 the superficial and deep capillary plexus was reported. In their study, the measurements were done within

244 one week of discharge after complete recovery. Another OCTA based study reported several retinal
245 findings including hemorrhages, cotton wool spots, dilated veins, tortuous vessel and changes in mean
246 arterial and vein diameter in patients with COVID-19¹³. Although the authors stated that such findings
247 indicating microangiopathy might be secondary to COVID-19 or incidental, they also speculated that the
248 virus itself or the systemic treatments used might have triggered microangiopathy in patients with
249 systemic vascular disease. In the present study, all retinal and choroicapillaris changes were examined in
250 post-mortem tissue. We detect similar reduction in retinal vascular density in COVID-19 patients along
251 with increased vessel tortuosity, vein occlusions and hemorrhages. However, unlike the retinal
252 vasculature, the choroidal vasculature did not appear to be severely affected as a result of the COVID-19
253 infection. It is important to note that there are studies that have found little or no change in retinal
254 vascular density⁴¹. These apparent differences in reported observations, could be due to the disease
255 severity, study populations, diagnostic criteria and methodologies used in the different studies. It still
256 remains to be determined whether the changes in the retinal vasculature is due to a direct infection of the
257 retina or whether these are part of a common systemic vascular diseases such as diabetes mellitus, chronic
258 kidney disease and hypertension.

259 We also find evidence of increased microglial cells in the retina of the COVID-19 eyes. There is
260 no reported evidence yet for increased infiltration of inflammatory cells in the retina, though a recent case
261 study reported a possible association between COVID-19 and Papillophlebitis, a rare condition that
262 occurs due to a consequence of inflammation of the retinal vein⁴². Chronological aging is associated with
263 a significant increase in the total numbers of both hypertrophic as well as dystrophic microglia. A recent
264 study showed that dystrophy are the disease associated microglia morphology²¹. In the present study we
265 see evidence for increased microglial cells in the COVID-19 eyes and several of these appear to show the
266 characteristic of microglial dystrophy and hypertrophy. Hypertrophic microglia are associated with
267 increased microglial activation. However, due to the very low numbers of eyes examined and the
268 subjectivity associated with classifying a hypertrophic, dystrophic and normal microglia purely based on
269 morphological attributes, it is difficult to infer whether these dystrophic/hypertrophic morphological

270 features is associated with changes in the microglia. While there is likely more than one explanation for
271 the differences detected in the microglial morphology, whether this is a direct consequence of the SARS-
272 CoV-2 infection remains to be determined. However, these preliminary findings are interesting and
273 suggest that there could be an increase in the secretion of the pro-inflammatory molecules as a result of
274 the microglial dystrophy and warrant further investigation. Though, there is no report on activation of
275 microglia in the retina, there is some evidence from neuropathological findings in patients who have died
276 from COVID-19 that in a significant number of these patients, various gliosis stages with diffuse
277 activation of microglia and astrocytes could be detected. In our study we also find evidence of increased
278 astrocyte activation as indicated by the increase in GFAP immunoreactivity. The astrocyte morphology
279 also appears to be different with more elongated morphology closer to the ONH and dense mesh like
280 networks toward the middle and the periphery. Such phenotypic heterogeneity has been associated with
281 different responses of the astrocytes to an injury and their adaptive functions. Importantly, the dense mesh
282 like network is indicative of scar formation after an injury^{43,44}. GFAP has been also detected in the plasma
283 of patients with COVID-19 and the amount is directly correlated with the severity of the disease^{45,46}.
284 Whether the observed activation is temporary and is resolved after the infection is gone, remains to be
285 seen. However, even short-term increase in GFAP can be detrimental to the underlying neuronal cells and
286 can result in focal damage. Despite the small sample size, the work presented here raises the possibility
287 of subclinical vascular deficits combined with increased inflammation in patients with severe disease who
288 have recovered from COVID-19 infection.

289 This study has some limitations, including the small sample size and the broad inclusion criteria.
290 The severity of the viral infection is unknown, and the duration of hospitalization could severely impact
291 the histopathological findings, thus limiting the generalization of the findings. Owing to the small
292 numbers of available control eyes available, the cause of death for these control cohorts will notably have
293 a huge impact on all the assessments reported. All care was taken to ensure that the investigated cohorts
294 were closely matched in terms of age as well as the duration that these patients were maintained on
295 ventilators. These limitations do not appear to change the results as many of the reported findings could

296 only be observed in the deceased patients with COVID-19. Further evaluation with a much larger sample
297 size is needed to determine the effects of SAR-CoV-2 infection on retinal morphology, vasculature,
298 inflammation and gliosis.

299 In conclusion, we observed several ocular anomalies the COVID-19 cohorts compared to the
300 control cohorts. Surprisingly, despite the small sample size, there were some consistent differences
301 detected between the patient cohorts and the COVID-19 negative patients. Of note are the subclinical
302 microvasculature features that we observed. As some of these observations have not been noted
303 previously these histopathological analyses of the post-mortem eyes from the COVID-19 patients suggest
304 that as more individuals recover from the COVID-19 infections, depending on the severity of their illness
305 these individuals may present with ocular clinical symptoms that have not been examined previously.
306 Therefore, a heightened vigilance for the long -term disease sequelae in other tissues like the eye is
307 warranted.

308

309 **ACKNOWLEDGMENTS**

310 This research was funded by grants from the U.S. National Institutes of Health/National Eye Institute
311 EY027077-01 (S.R.), RPB1503 (S.R.), EY027750 (VLB), a National Eye Institute P30-EY025585 Core
312 Grant, a Cleveland Eye Bank Foundation Grant awarded to the Cole Eye Institute, and Research to Prevent
313 Blindness Challenge Grant. Research activities at Eversight are supported by funding from LC Industries
314 (Durham, NC), Eye Bank Association of America and Connecticut Lions Eye Research Foundation. The
315 authors declare no conflicts of interest.

316

317 **AUTHORS CONTRIBUTIONS**

318 VLB, and SR contributed to study conception and design, and accessed and verified the data. VKJ drafted
319 the manuscript. All authors contributed to data acquisition, interpreted the data, critically revised the
320 manuscript, and provided approval for the final version of the manuscript to be published.

321

322 **FINANCIAL DISCLOSURE(S)**

323 None.

324

325

326

327 **FIGURE LEGENDS**

328

329 **Figure 1.** Ex-vivo imaging of COVID-19 donor eyes. Representative fundus (**A-F**) and SLO images (**G-**

330 **L**) collected from COVID-19 and an age-similar controls. Fovea (black arrow) and optic nerve head (ON)

331 were visible in all eyes. Hemorrhage spots (white arrowheads) were visible in most of the COVID-19

332 eyes. BAF images of COVID-19 (**H, J, L**) and control (**G, I, K**) eyes revealed a pattern that matched the

333 fundus images. Also, in the COVID-19 eyes, the detached retinas were apparent with SLO (**H, J, L, ***).

334 Mean intensity calculation using BAF SLO images with all age groups (**M**), age group 80-90 (**N**), age

335 group 70-75 (**O**), and age group < 45 (**P**). Scale bar A-F= 0.3cm, G-L= 200 μ m.

336

337 **Figure 2.** Histology and immunohistology of COVID-19 donor eyes. Representative toluidine blue-

338 stained plastic 1 μ m sections of retinas from COVID-19 donors (**B, D, E, F**) and an age-similar controls

339 (**A, C**). Morphology of the control retina displayed typical retinal lamina. A few control retinas displayed

340 cystoid degeneration (**C**) in the far periphery, while these were observed in the central retina of several

341 COVID-19 eyes (**D**). Two of the COVID-19 retinas showed a cotton-wool exudate (**E, F, asterisk**) in the

342 outer plexiform layer close to the optic nerve head. Immunofluorescence of two COVID-19 retinas

343 labeled with antibodies to SARS-CoV S protein (**H-I**, Alexa488, green) showed the presence of several

344 positive cells (arrows) when compared to control (**G**). GCL ganglion cell layer, INL inner nuclear layer,

345 ONL outer nuclear layer, POS photoreceptor outer segments, RPE retinal pigment epithelium, Ch

346 Choroid. Scale bar A-D, F= 50 μ m, E= 100 μ m, G-I= 40 μ m.

347 **Figure 3.** Retinal vascular abnormalities in COVID-19 patients. Representative images of retinal
348 vasculature visualized using rhodamine-conjugated UEA lectin to label the blood vessels. (A-R).
349 Representative images are from three different age groups. Age group 80-90 (A-F), Age group 70-75 (G-
350 L) and age group <45 (M-R). To illustrate the spatial differences in vascular density of the retinal
351 microvasculature, the retinal preparations were subdivided into three different zones, one near the optic
352 nerve head closer to the vein (A,D,G,J,M,P) one near the middle closer to the vein (B,E,H,K,N,Q) and one
353 between the middle and the periphery (C,F,I,L,O,R). Vessel density was severely reduced together with
354 several capillaries showing signs of atrophy(white arrowheads) in the eyes from the COVID 19 patients (E,
355 F, L, R, Q) compared to age matched controls (B, C, I, O, N). Most noticeable difference were observed
356 in regions distal to the optic nerve head however in one of the COVID positive sample (P-R), regressing
357 vessels could be detected in the entire retina. White arrowheads indicate the severe capillary dropout. ONH,
358 Optic nerve head, V, Vein, Mid, Middle region, Scale bar: 100um.

359
360 **Figure 4.** Retinal vascular anomalies are accompanied by gliosis and inflammation. Retinal whole mounts
361 stained with an antibody for GFAP for glial cells (A- L; green) and Iba1 for microglia (A'-L', grey). There
362 is an overall increase in GFAP immunoreactivity near the ONH regions (G,K) in the COVID-19 patients
363 when compared to age matched controls (E, I). However, in one COVID negative case (A, B) there is a
364 similar increase in GFAP immunoreactivity near the ONH area (A), but not near the middle regions (B). In
365 general the GFAP positive cells appear to form dense networks and overlapping cable like structures
366 indicative of increased gliosis (A'-L') Representative images of retinal tissues stained with Iba1 to visualize
367 the microglial cells. In all the COVID positive eyes, in the regions distal to the optic nerve and right next
368 to the vein. (C', D' G' H'K' L') there is an increase in the total number of microglial cells irrespective of
369 the age of the deceased patient compared to the control eyes (B',F',J'). In general, in all of the eyes
370 examined, several of the microglial cells displayed hypertrophic morphology (red arrowhead, D'-L') with
371 some showing fragmented processes (black arrowhead A', B', G', H', L'), beady, processes (blue
372 arrowheads, K', L') indicative of dystrophic microglia with very few normal looking microglia only seen

373 in one eye examined (Magenta arrowheads, C',D'). ONH, Optic nerve head, V, Vein, Mid, Middle region,

374 Scale bar: 100um.

375
376

377

378

379

380

381

382

383

384

385

386 REFERENCES

387

- 388 1. Chen L, Deng C, Chen X, et al. Ocular manifestations and clinical characteristics of 534 cases of
389 COVID-19 in China: A cross-sectional study. *medRxiv*. 2020:2020.2003.2012.20034678.
- 390 2. Abrishami M, Tohidinezhad F, Daneshvar R, et al. Ocular Manifestations of Hospitalized Patients
391 with COVID-19 in Northeast of Iran. *Ocul Immunol Inflamm*. 2020;28(5):739-744.
- 392 3. Hong N, Yu W, Xia J, Shen Y, Yap M, Han W. Evaluation of ocular symptoms and tropism of SARS-
393 CoV-2 in patients confirmed with COVID-19. *Acta Ophthalmol*. 2020.
- 394 4. Cheema M, Aghazadeh H, Nazarali S, et al. Keratoconjunctivitis as the initial medical
395 presentation of the novel coronavirus disease 2019 (COVID-19). *Can J Ophthalmol*.
396 2020;55(4):e125-e129.
- 397 5. Yordi S, Ehlers JP. COVID-19 and the eye. *Cleve Clin J Med*. 2020.
- 398 6. Jin YP, Trope GE, El-Defrawy S, Liu EY, Buys YM. Ophthalmology-focused publications and
399 findings on COVID-19: A systematic review. *Eur J Ophthalmol*. 2021:1120672121992949.
- 400 7. Zhou L, Xu Z, Castiglione GM, Soiberman US, Eberhart CG, Duh EJ. ACE2 and TMPRSS2 are
401 expressed on the human ocular surface, suggesting susceptibility to SARS-CoV-2 infection. *Ocul*
402 *Surf*. 2020;18(4):537-544.
- 403 8. Leonardi A, Rosani U, Brun P. Ocular Surface Expression of SARS-CoV-2 Receptors. *Ocul Immunol*
404 *Inflamm*. 2020;28(5):735-738.
- 405 9. Wagner J, Jan Danser AH, Derkx FH, et al. Demonstration of renin mRNA, angiotensinogen
406 mRNA, and angiotensin converting enzyme mRNA expression in the human eye: evidence for an
407 intraocular renin-angiotensin system. *Br J Ophthalmol*. 1996;80(2):159-163.
- 408 10. Casagrande M, Fitzek A, Spitzer MS, et al. Presence of SARS-CoV-2 RNA in the Cornea of Viremic
409 Patients With COVID-19. *JAMA Ophthalmol*. 2021.
- 410 11. Sawant OB, Singh S, Wright RE, 3rd, et al. Prevalence of SARS-CoV-2 in human post-mortem
411 ocular tissues. *Ocul Surf*. 2021;19:322-329.
- 412 12. Abrishami M, Emamverdian Z, Shoeibi N, et al. Optical coherence tomography angiography
413 analysis of the retina in patients recovered from COVID-19: a case-control study. *Can J*
414 *Ophthalmol*. 2021;56(1):24-30.
- 415 13. Invernizzi A, Torre A, Parrulli S, et al. Retinal findings in patients with COVID-19: Results from the
416 SERPICO-19 study. *EClinicalMedicine*. 2020;27:100550.

- 417 14. Bonilha VL, Rayborn ME, Bell BA, Marino MJ, Fishman GA, Hollyfield JG. Retinal Histopathology
418 in Eyes from a Patient with Stargardt disease caused by Compound Heterozygous ABCA4
419 Mutations. *Ophthalmic Genet.* 2015;1-11.
- 420 15. Bonilha VL, Shadrach KG, Rayborn ME, et al. Retinal deimination and PAD2 levels in retinas from
421 donors with age-related macular degeneration (AMD). *Exp Eye Res.* 2013;111:71-78.
- 422 16. Edwards MM, Bonilha VL, Bhutto IA, et al. Retinal Glial and Choroidal Vascular Pathology in
423 Donors Clinically Diagnosed With Stargardt Disease. *Invest Ophthalmol Vis Sci.* 2020;61(8):27.
- 424 17. Stokoe NL, Turner RW. Normal retinal vascular pattern. Arteriovenous ratio as a measure of
425 arterial calibre. *Br J Ophthalmol.* 1966;50(1):21-40.
- 426 18. Alam M, Toslak D, Lim JI, Yao X. Color Fundus Image Guided Artery-Vein Differentiation in
427 Optical Coherence Tomography Angiography. *Invest Ophthalmol Vis Sci.* 2018;59(12):4953-4962.
- 428 19. Bagheri N, Bell BA, Bonilha VL, Hollyfield JG. Imaging human postmortem eyes with SLO and
429 OCT. *Adv Exp Med Biol.* 2012;723:479-488.
- 430 20. Streit WJ, Sammons NW, Kuhns AJ, Sparks DL. Dystrophic microglia in the aging human brain.
431 *Glia.* 2004;45(2):208-212.
- 432 21. Shahidehpour RK, Higdon RE, Crawford NG, et al. Dystrophic microglia are a disease associated
433 microglia morphology in the human brain. *bioRxiv.* 2020:2020.2007.2030.228999.
- 434 22. Conde JR, Streit WJ. Microglia in the aging brain. *J Neuropathol Exp Neurol.* 2006;65(3):199-203.
- 435 23. Miller KR, Streit WJ. The effects of aging, injury and disease on microglial function: a case for
436 cellular senescence. *Neuron Glia Biol.* 2007;3(3):245-253.
- 437 24. Ulhaq ZS, Soraya GV. The prevalence of ophthalmic manifestations in COVID-19 and the
438 diagnostic value of ocular tissue/fluid. *Graefes Arch Clin Exp Ophthalmol.* 2020;258(6):1351-
439 1352.
- 440 25. Wu P, Duan F, Luo C, et al. Characteristics of Ocular Findings of Patients With Coronavirus
441 Disease 2019 (COVID-19) in Hubei Province, China. *JAMA Ophthalmol.* 2020;138(5):575-578.
- 442 26. Ocansey S, Abu EK, Abraham CH, et al. Ocular Symptoms of SARS-CoV-2: Indication of Possible
443 Ocular Transmission or Viral Shedding. *Ocul Immunol Inflamm.* 2020;28(8):1269-1279.
- 444 27. Casagrande M, Fitzek A, Puschel K, et al. Detection of SARS-CoV-2 in Human Retinal Biopsies of
445 Deceased COVID-19 Patients. *Ocul Immunol Inflamm.* 2020;28(5):721-725.
- 446 28. Seah I, Agrawal R. Can the Coronavirus Disease 2019 (COVID-19) Affect the Eyes? A Review of
447 Coronaviruses and Ocular Implications in Humans and Animals. *Ocul Immunol Inflamm.*
448 2020;28(3):391-395.
- 449 29. Marinho PM, Marcos AAA, Romano AC, Nascimento H, Belfort R, Jr. Retinal findings in patients
450 with COVID-19. *Lancet.* 2020;395(10237):1610.
- 451 30. Pereira LA, Soares LCM, Nascimento PA, et al. Retinal findings in hospitalised patients with
452 severe COVID-19. *Br J Ophthalmol.* 2020.
- 453 31. Mansour AM, Jampol LM, Logani S, Read J, Henderly D. Cotton-wool spots in acquired
454 immunodeficiency syndrome compared with diabetes mellitus, systemic hypertension, and
455 central retinal vein occlusion. *Arch Ophthalmol.* 1988;106(8):1074-1077.
- 456 32. Mansour AM, Jampol LM, Hrisomalos NF, Greenwald M. Case report. Cavernous hemangioma of
457 the optic disc. *Arch Ophthalmol.* 1988;106(1):22.
- 458 33. Brown GC, Brown MM, Hiller T, Fischer D, Benson WE, Magargal LE. Cotton-wool spots. *Retina.*
459 1985;5(4):206-214.
- 460 34. McLeod D, Restori M, Wright JE. Rapid B-scanning of the vitreous. *Br J Ophthalmol.*
461 1977;61(7):437-445.
- 462 35. Scholl S, Kirchhof J, Augustin AJ. Pathophysiology of macular edema. *Ophthalmologica.* 2010;224
463 Suppl 1:8-15.
- 464 36. Rotsos TG, Moschos MM. Cystoid macular edema. *Clin Ophthalmol.* 2008;2(4):919-930.

- 465 37. Strong S, Liew G, Michaelides M. Retinitis pigmentosa-associated cystoid macular oedema:
466 pathogenesis and avenues of intervention. *Br J Ophthalmol.* 2017;101(1):31-37.
- 467 38. De Bats F, Wolff B, Vasseur V, et al. "En-face" spectral-domain optical coherence tomography
468 findings in multiple evanescent white dot syndrome. *J Ophthalmol.* 2014;2014:928028.
- 469 39. Zhang X, Zeng H, Bao S, Wang N, Gillies MC. Diabetic macular edema: new concepts in patho-
470 physiology and treatment. *Cell Biosci.* 2014;4:27.
- 471 40. Turker IC, Dogan CU, Guven D, Kutucu OK, Gul C. Optical coherence tomography angiography
472 findings in patients with COVID-19. *Can J Ophthalmol.* 2021.
- 473 41. Savastano MC, Gambini G, Cozzupoli GM, et al. Retinal capillary involvement in early post-
474 COVID-19 patients: a healthy controlled study. *Graefes Arch Clin Exp Ophthalmol.* 2021.
- 475 42. Insausti-Garcia A, Reche-Sainz JA, Ruiz-Arranz C, Lopez Vazquez A, Ferro-Osuna M.
476 Papillophlebitis in a COVID-19 patient: Inflammation and hypercoagulable state. *Eur J*
477 *Ophthalmol.* 2020:1120672120947591.
- 478 43. Wanner IB, Anderson MA, Song B, et al. Glial scar borders are formed by newly proliferated,
479 elongated astrocytes that interact to corral inflammatory and fibrotic cells via STAT3-dependent
480 mechanisms after spinal cord injury. *J Neurosci.* 2013;33(31):12870-12886.
- 481 44. Burda JE, Sofroniew MV. Reactive gliosis and the multicellular response to CNS damage and
482 disease. *Neuron.* 2014;81(2):229-248.
- 483 45. Kanberg N, Ashton NJ, Andersson LM, et al. Neurochemical evidence of astrocytic and neuronal
484 injury commonly found in COVID-19. *Neurology.* 2020;95(12):e1754-e1759.
- 485 46. Virhammar J, Naas A, Fallmar D, et al. Biomarkers for central nervous system injury in
486 cerebrospinal fluid are elevated in COVID-19 and associated with neurological symptoms and
487 disease severity. *Eur J Neurol.* 2020.

488

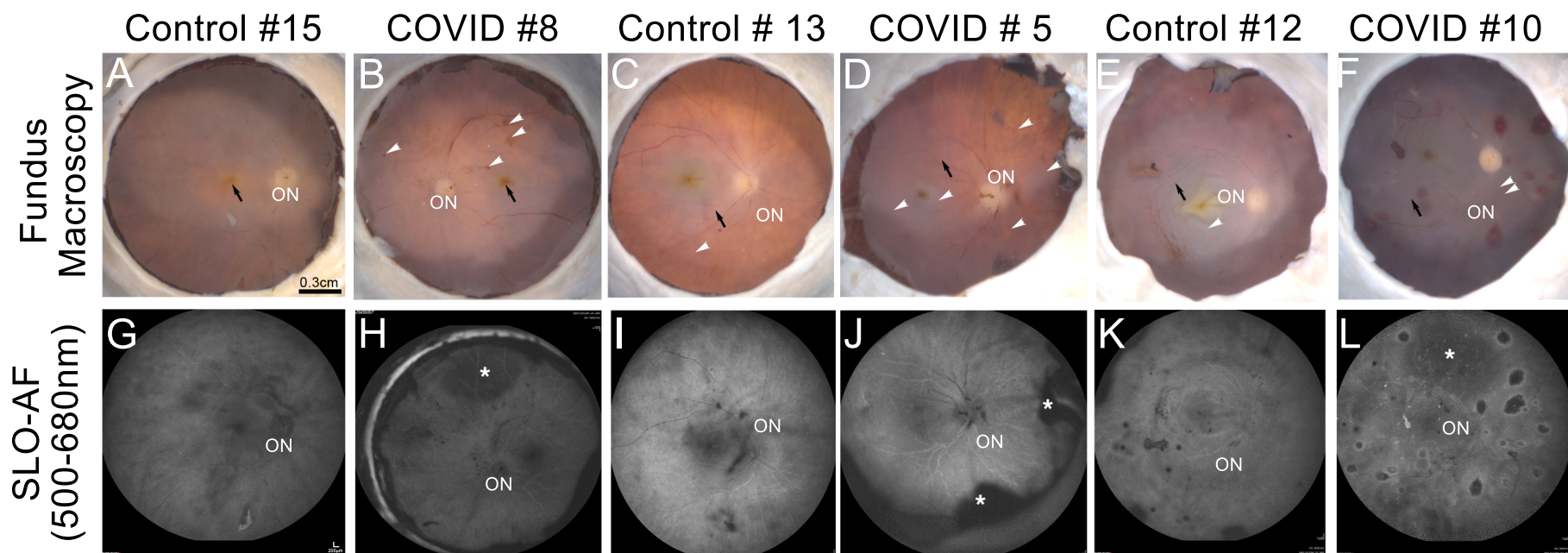


Table 1. Human Donor Information.

CASE	Age Range ^b	Gender ^c	Race ^d	PMI ^e	SARS-CoV-2 Testing
N ^a					
2	80-90	F	C	12	Positive ^f
4	60-65	M	SA	7	Positive ^f
5	70-75	F	C	27	Positive ^f
6	65-70	M	H	20	Positive ^f
7	55-60	F	C	11	Positive ^f
8	80-90	F	H	16	Positive ^f
10	45-50	M	H	13	Positive ^f
11	75-80	M	C	5	Negative
12	35-40	F	C	17	Negative
13	70-75	M	C	7	Negative
15	80-90	M	C	24	Negative
16	60-65	F	C	13	Negative
17	60-65	M	C	7	Negative

^a Cornea and anterior segments analysis were reported in Sawant et al., *Ocul Surf.* 2020 Nov 8;S1542-0124(20)30168-3. doi: 10.1016/j.jtos.2020.11.002.

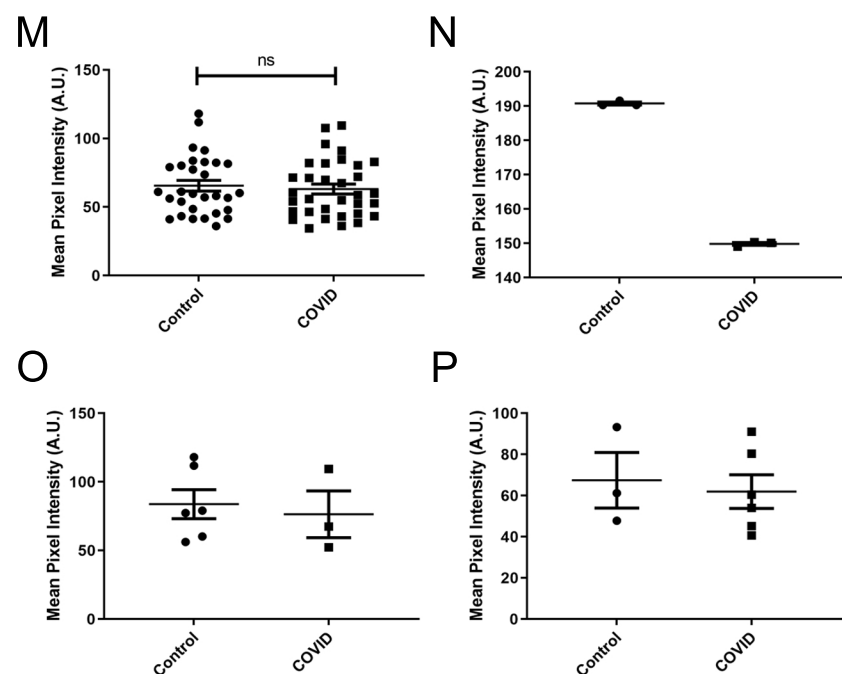
^b Age: age at death (years);

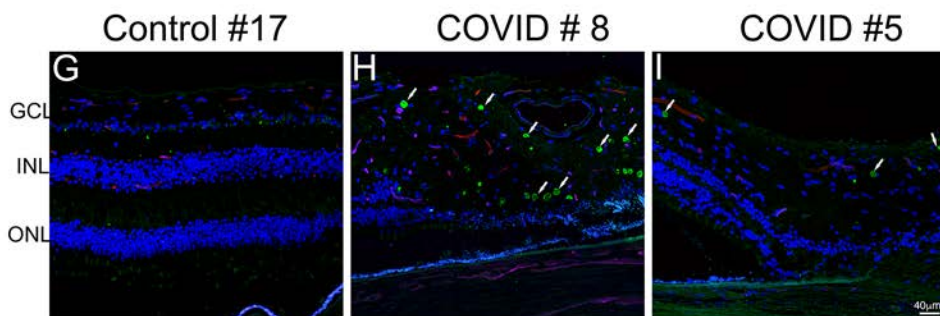
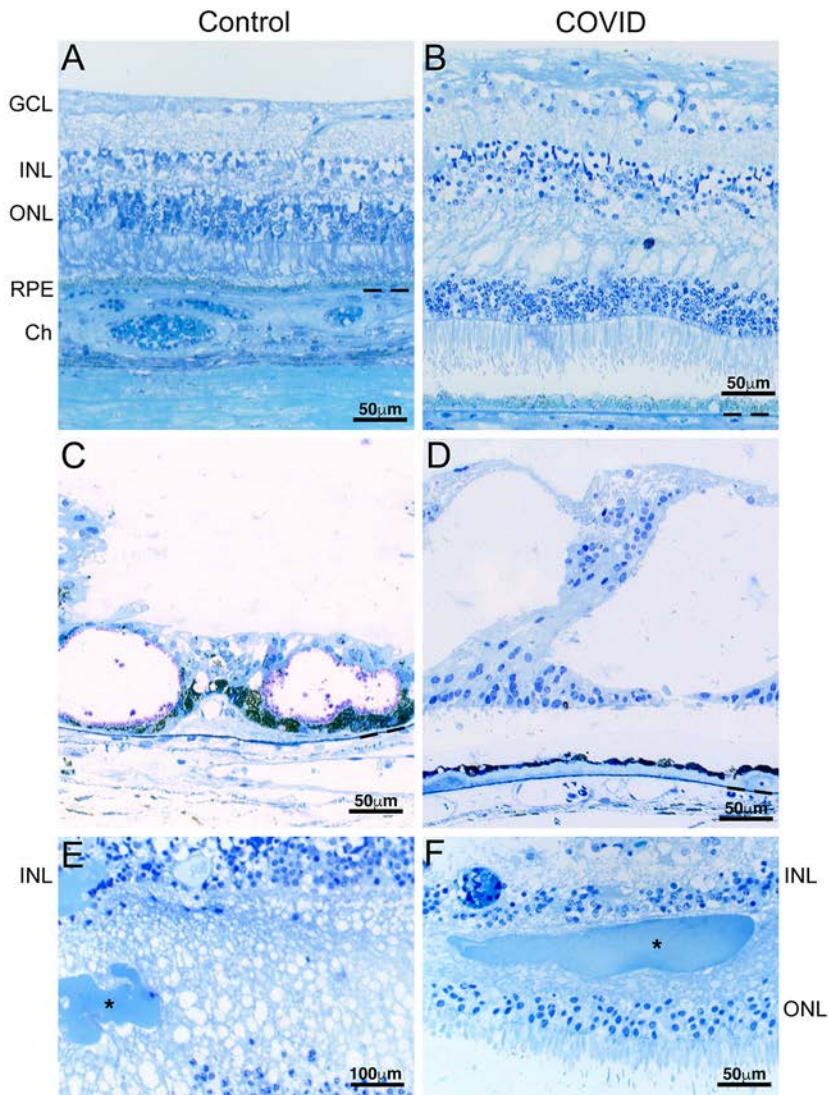
^c Gender: M = male, F = female;

^d Race: AA = African American, C = caucasian, H = hispanic, SA = south asian

^e Interval from death to preservation (hrs).

^f Results reported in Sawant et al., *Ocul Surf.* 2020 Nov 8;S1542-0124(20)30168-3. doi: 10.1016/j.jtos.2020.11.002.

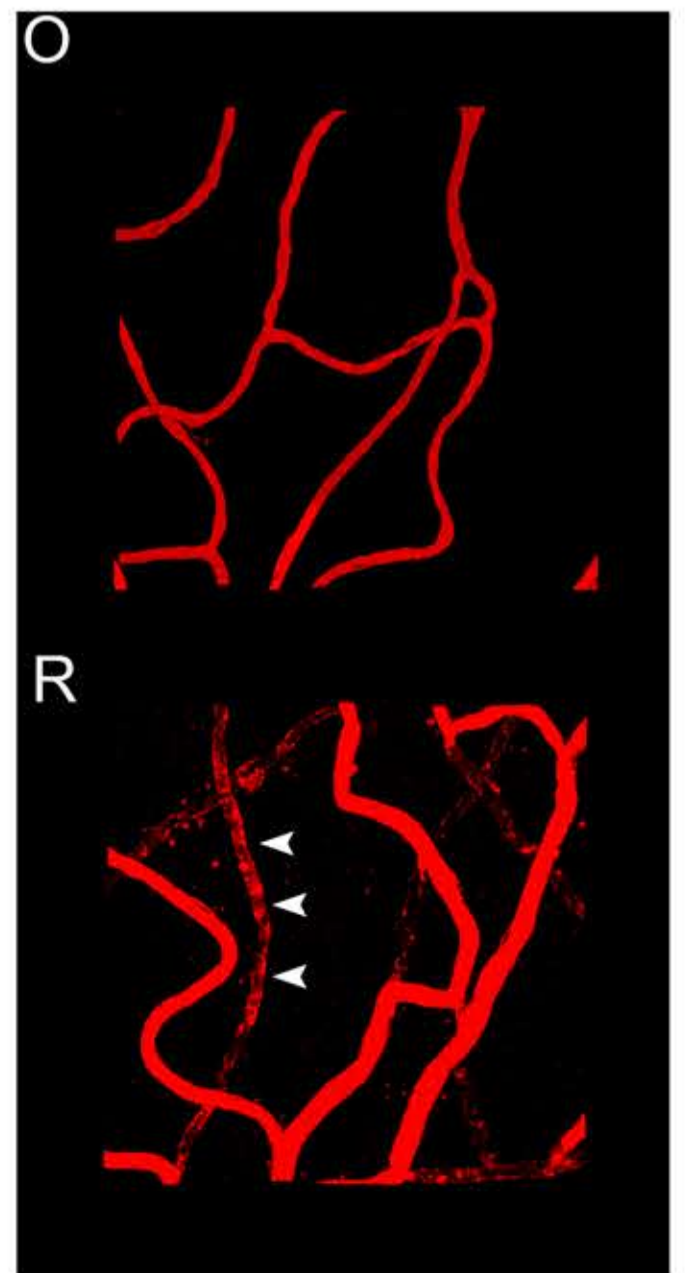
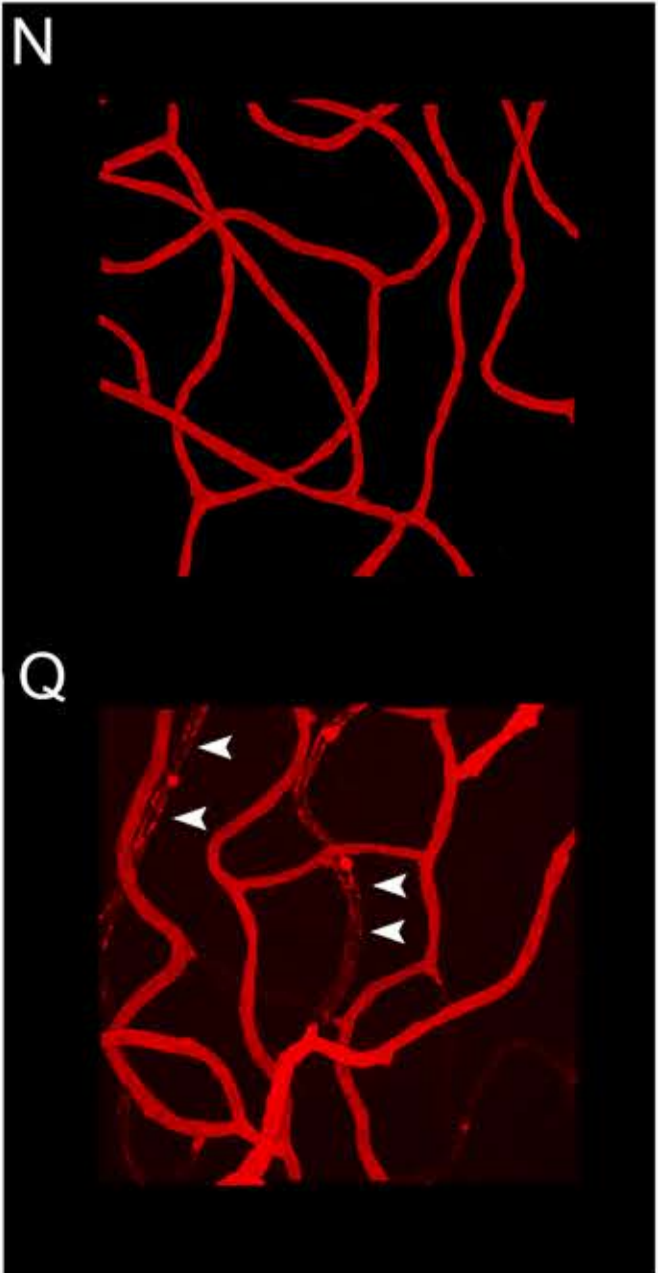
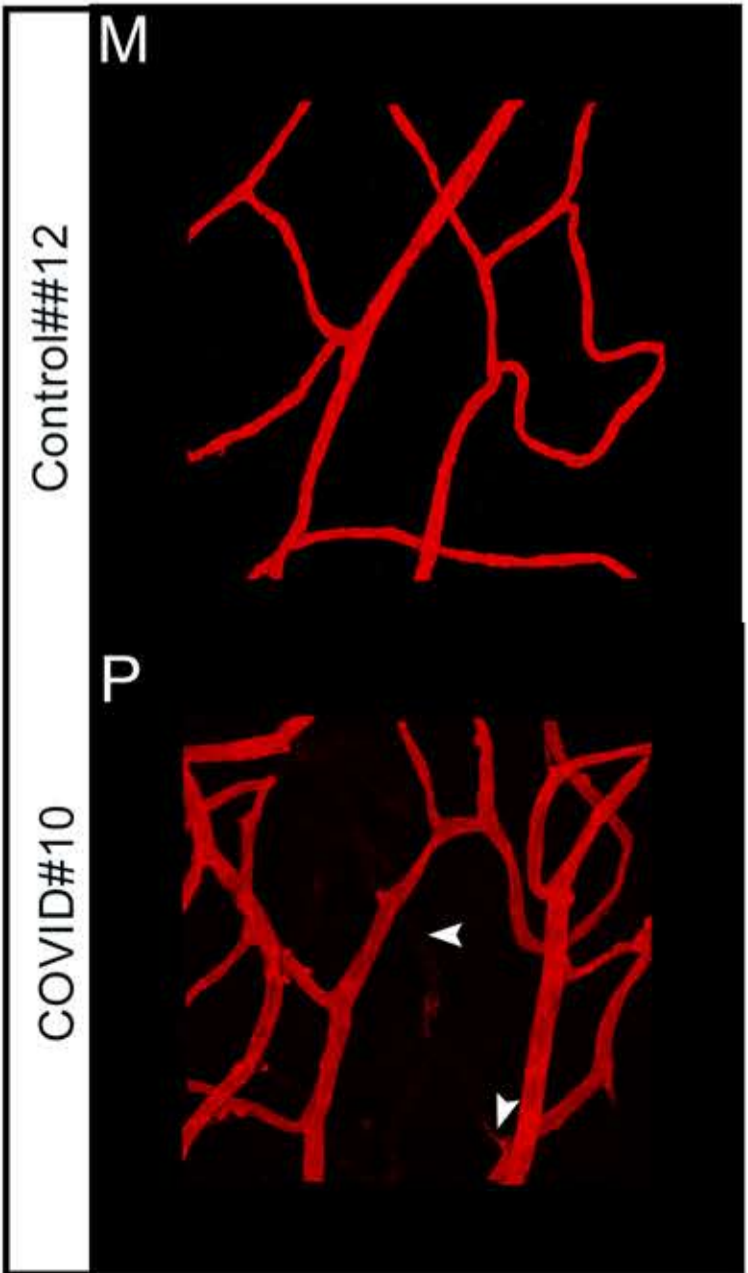
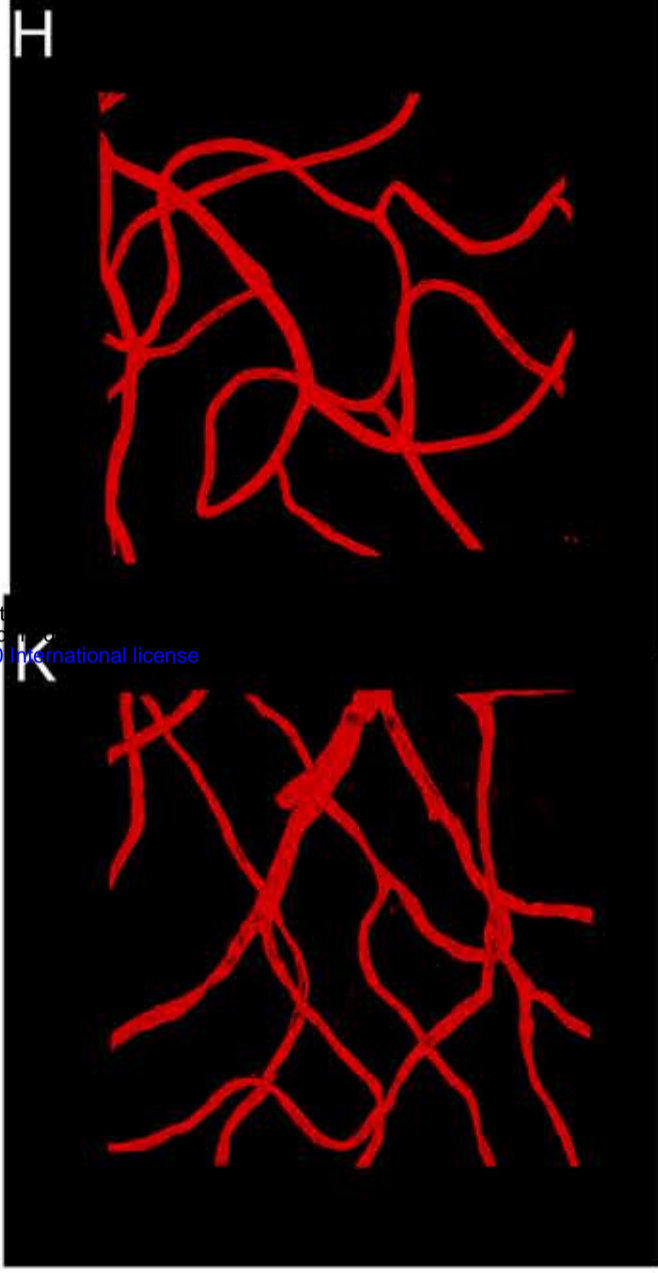
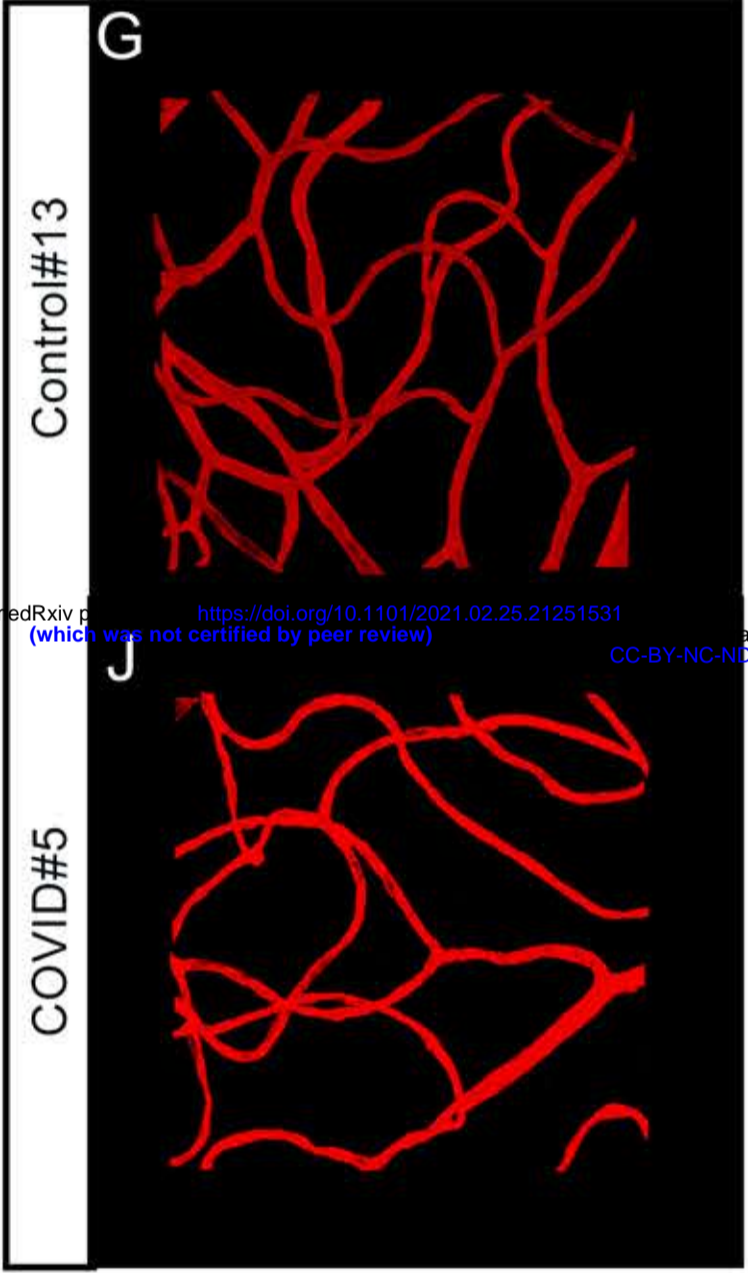
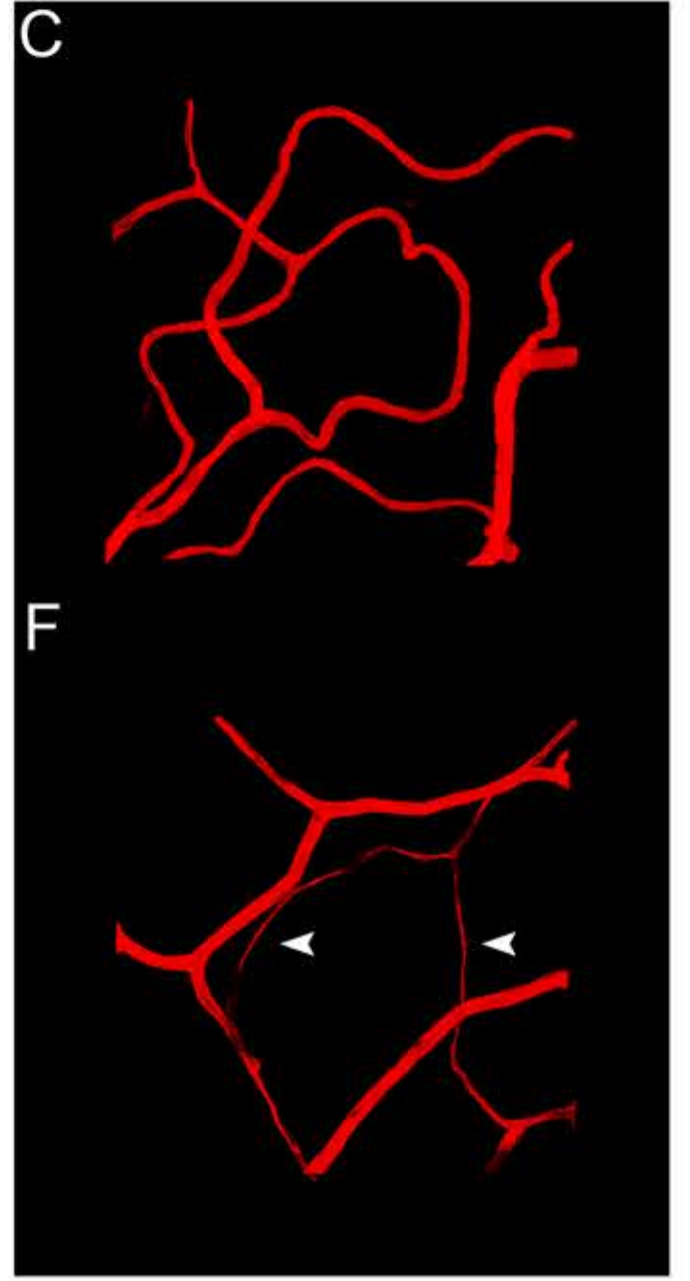
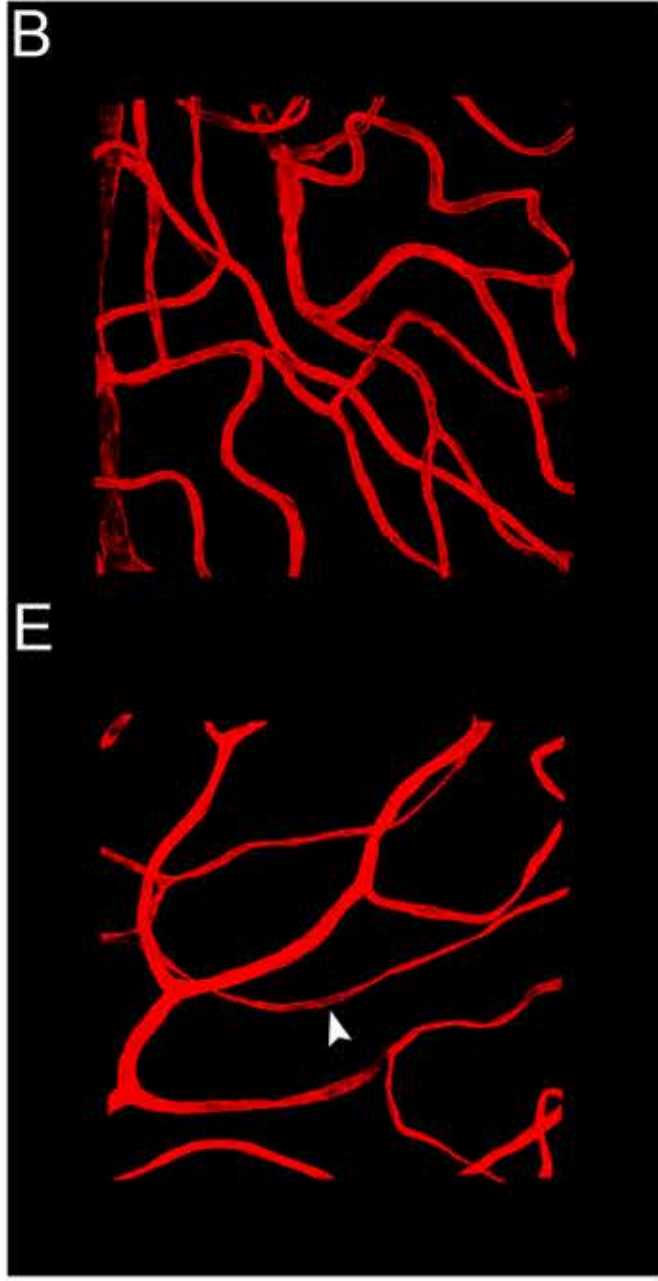
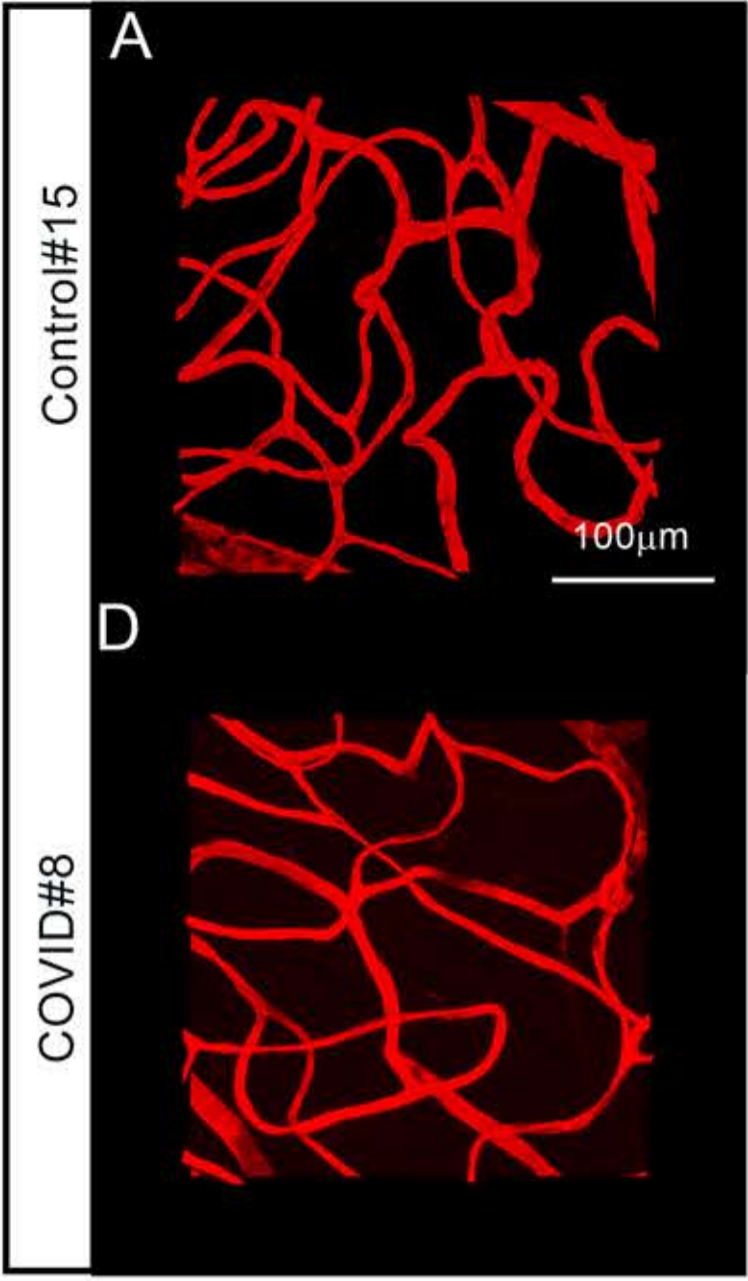




ONH/V

Mid/V

Mid



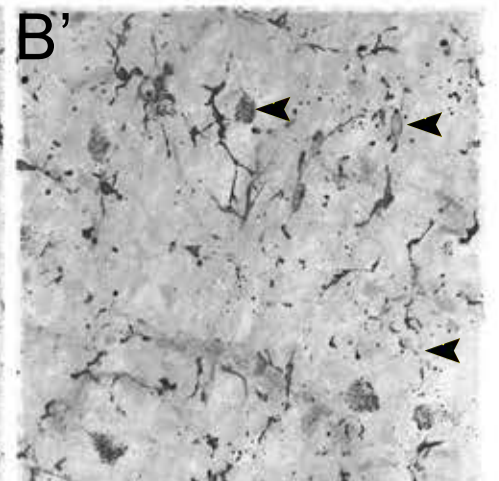
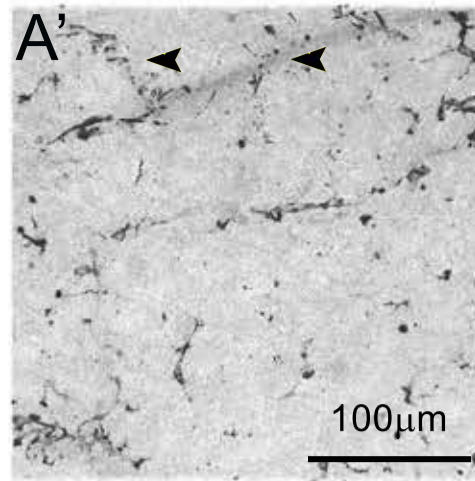
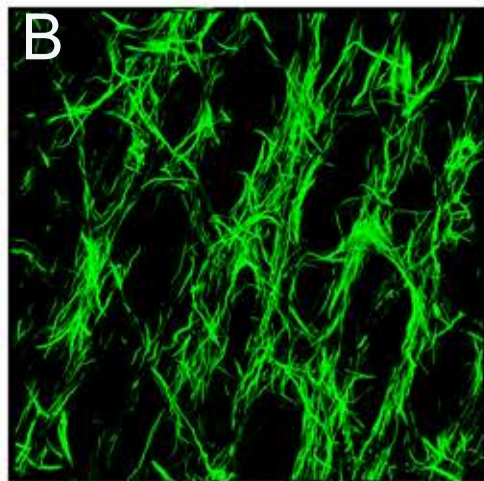
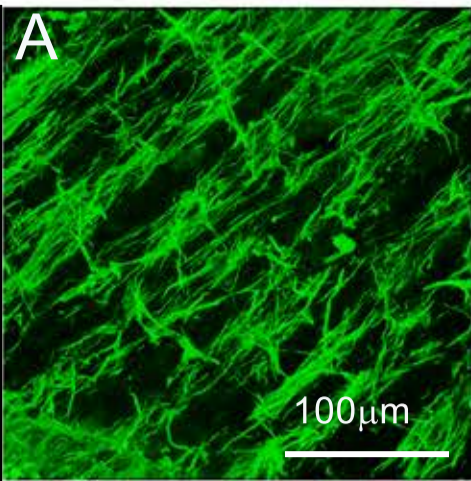
ONH/V

Mid/V

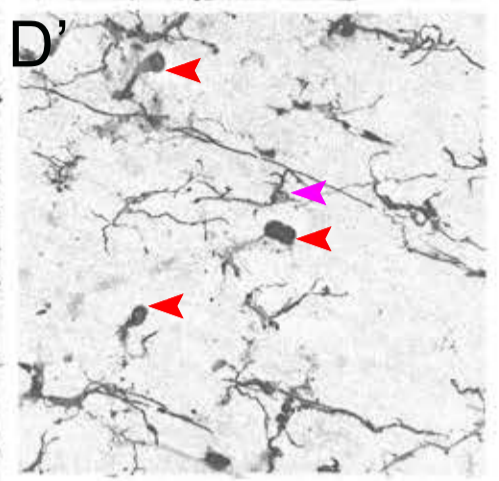
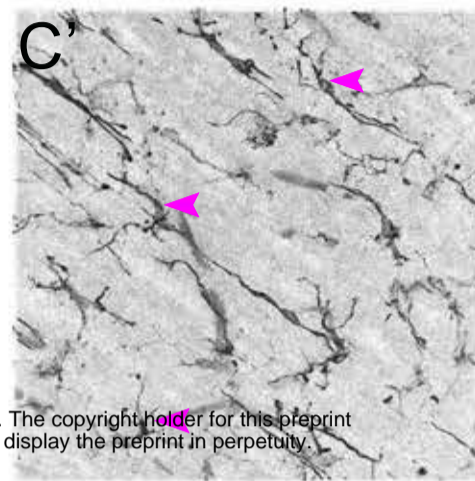
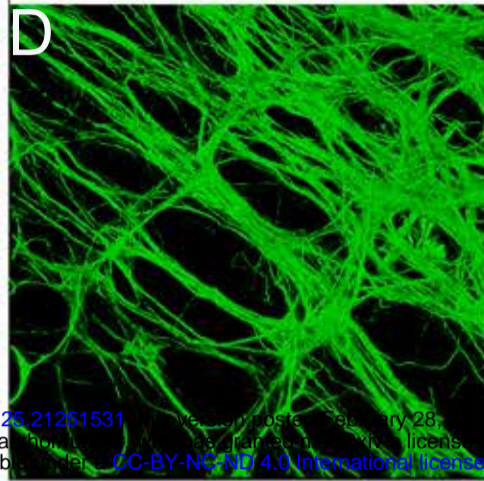
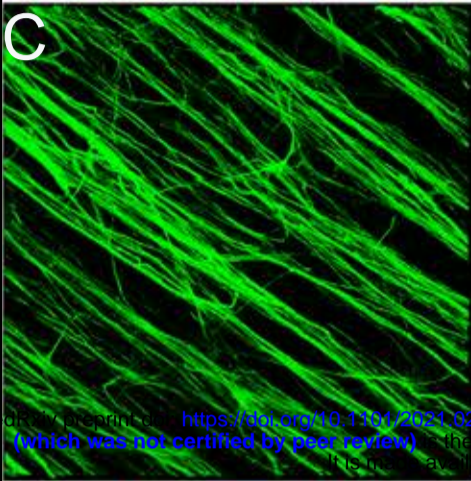
ONH/V

Mid/V

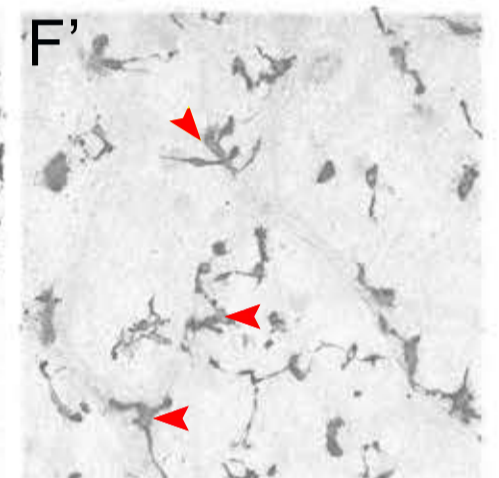
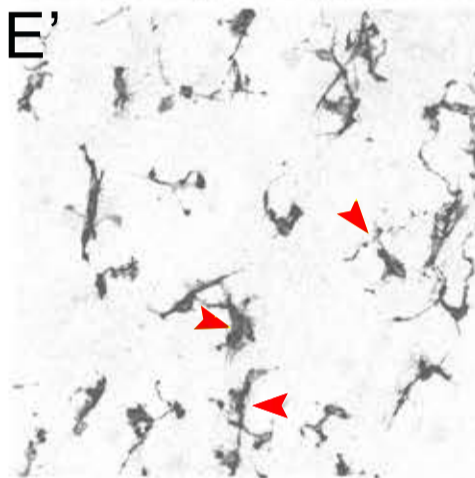
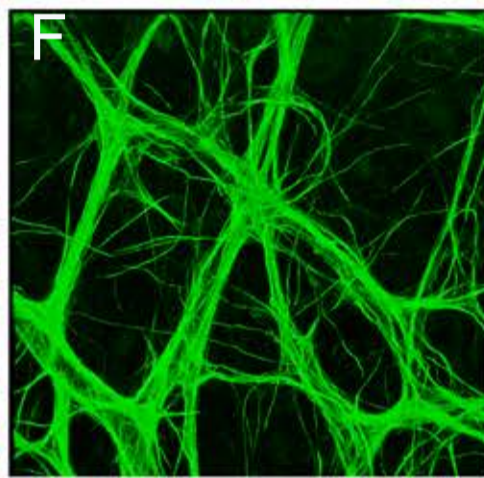
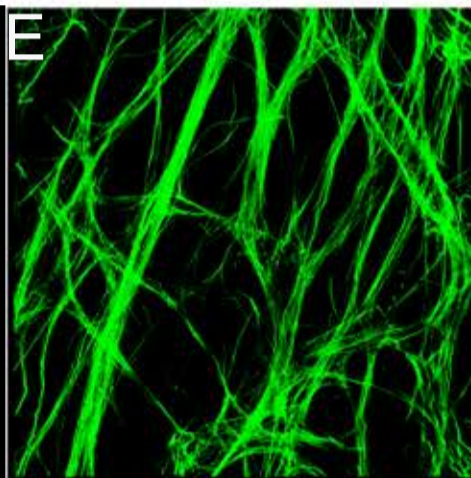
Control#15



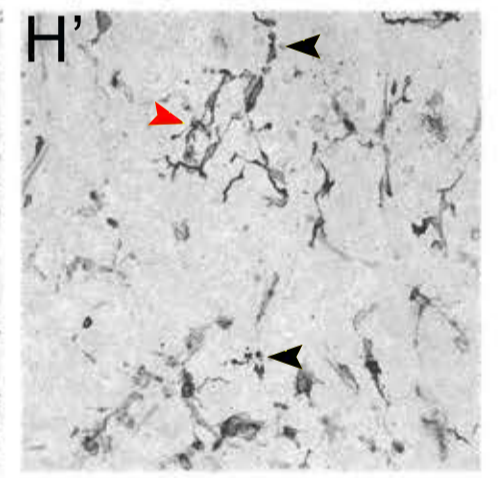
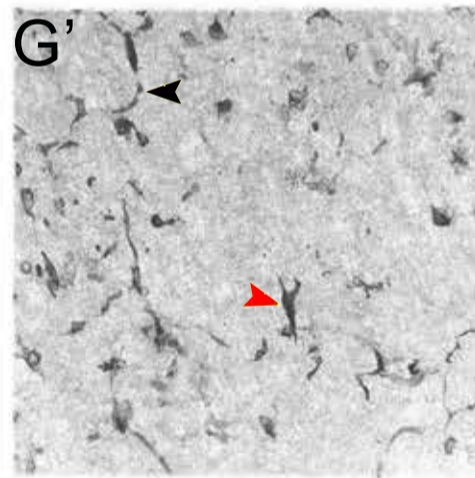
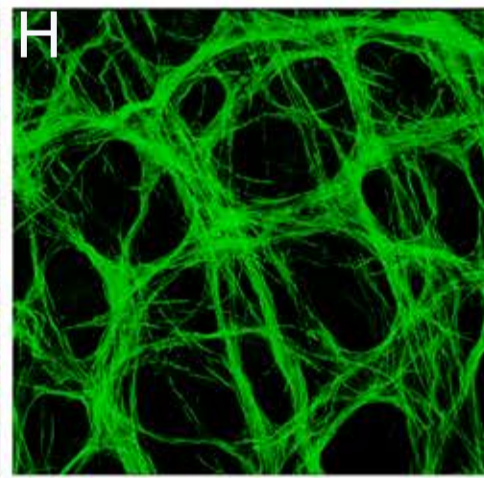
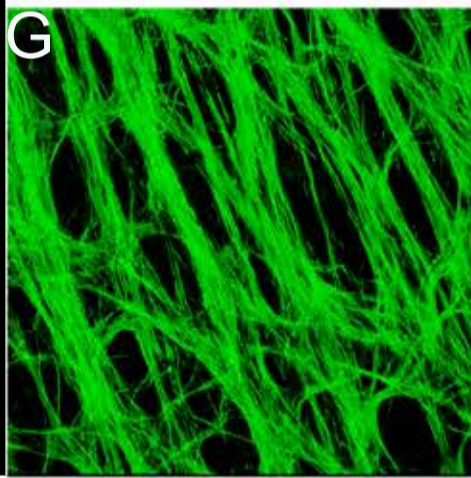
COVID#8



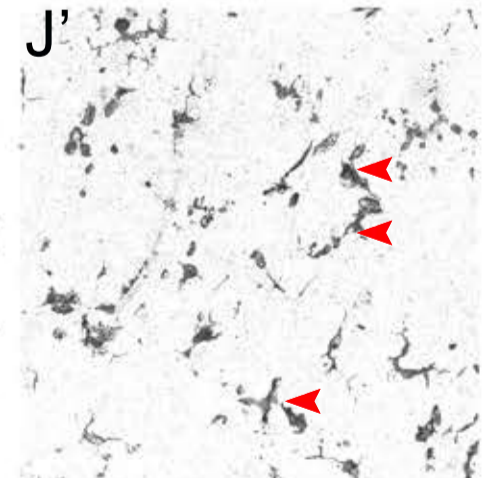
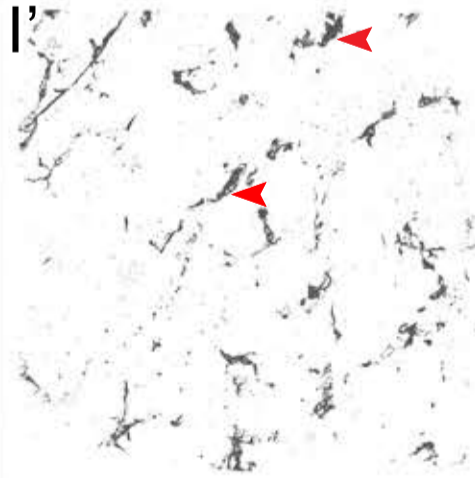
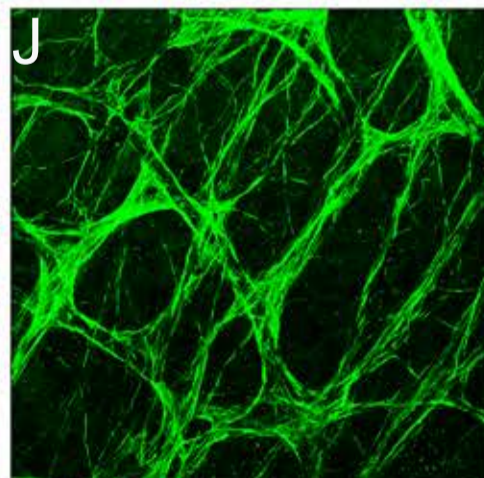
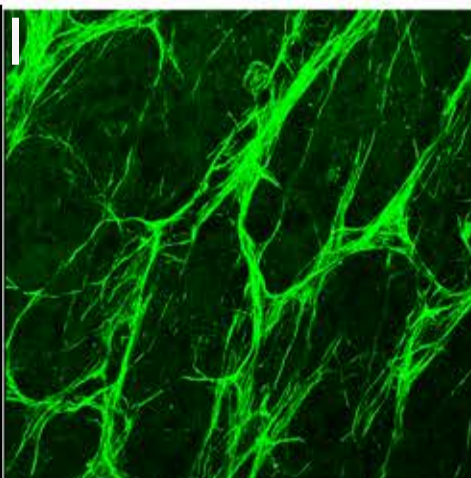
Control#13



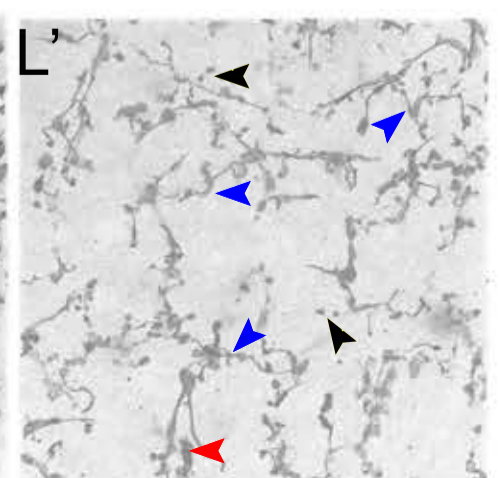
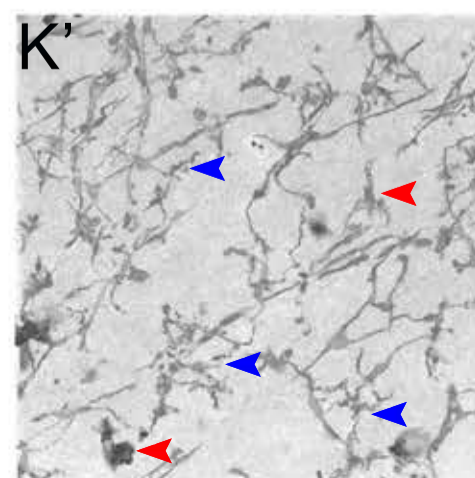
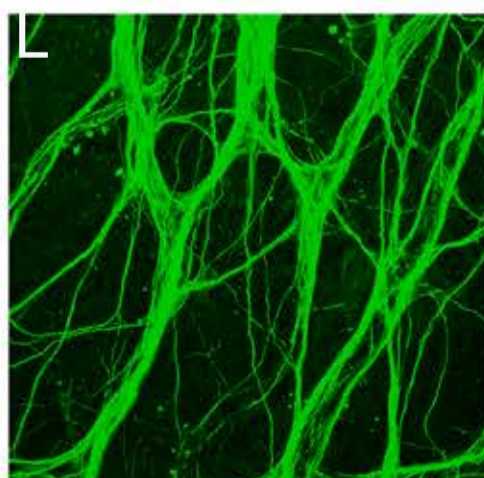
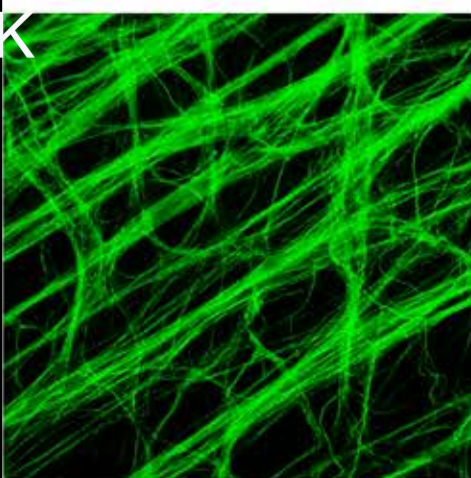
COVID#5



Control#12



COVID#10



medRxiv preprint doi: <https://doi.org/10.1101/2021.02.25.21251531>; this version posted February 28, 2021. The copyright holder for this preprint (which was not certified by peer review) is the author/funder, who has granted medRxiv a license to display the preprint in perpetuity. It is made available under a CC-BY-NC-ND 4.0 International license.

The copyright holder for this preprint (which was not certified by peer review) is the author/funder, who has granted medRxiv a license to display the preprint in perpetuity. It is made available under a CC-BY-NC-ND 4.0 International license.

Table 2. Assessment of retinal fundus and histological findings in donor eyes.

CASE N°	Hemorrhages ^a	Cystoid Degeneration ^b	Increased GFAP Staining	Increased infiltration of Iba-1+ cells	Central vein occlusion
2	Not Observed	X	X	X	Not observed
4	X	X	X	X	X
5	X		X	X	X ^e
6	Not Observed	X	X	X ^d	X ^f
7	X		X	X	X ^f
8	X		X	X	X
10	X	X	X	X	X
11	X	X	Not observed	Not observed	Not observed
12	X	X	Not observed	Not observed	Not observed
13	Not Observed	X	Not observed	X ^d	Not observed
15	X	X	X ^c	X ^d	X
16	Not Observed	X	Not observed	Not observed	X ^f
17	X	X	X	X ^d	X ^f

^a In at least one of the eyes;

^b Observed in both epon-embedded sections and cryosections;

^c Slightly elevated GFAP staining observed near the optic nerve head but not towards the middle and the peripheral retina.

^d Higher numbers of Iba-1 positive cells detected in the middle and peripheral retina.

^e Vascular Tortuosity in arteries and veins and aneurysms.

^f Though vein occlusion was not evident, the vascular staining was patchy in the veins and venules.